IEEE Access
Multidisciplinary | Rapid Review | Open Access Journal

Received December 26, 2019, accepted February 5, 2020, date of publication February 24, 2020, date of current version March 3, 2020.

Digital Object Identifier 10.1109/ACCESS.2020.2975892

A Novel Bayesian Patch-Based Approach for Image Denoising

RASHID ALI[1], PENG YUNFENG[1], (Member, IEEE), AND ROOH UL AMIN[2]
[1]School of Computer and Communication Engineering, University of Science and Technology Beijing (USTB), Beijing 100083, China
[2]Faculty of Telecommunication and Information Engineering, University of Engineering and Technology, Taxila 47080, Pakistan

Corresponding author: Rashid Ali (b20150558@xs.ustb.edu.cn)

This work was supported by the GIT Key Lab Foundation under Grant 2003008002.

ABSTRACT Recently patch-based image denoising techniques have gained the attention of researchers as it is being used in numerous image denoising applications. This article is proposing a new Bayesian Patch-based image denoising algorithm using Quaternion Wavelet Transform (QWT) for grayscale images. In the proposed work, a patch model has been used instead of the Gibbs distribution based energy model. Experimental results indicate that the proposed algorithm effectively diminishes noise. The results of the developed approach are also compared with other efficient image denoising algorithms such as Expected Patch Log Likelihood (EPLL), Block-matching and 3D filtering (BM3D), Patch-Based Locally Optimal Wiener (PLOW), Weighted Nuclear Norm Minimization (WNNM), Hybrid Robust Bilateral Filter-Total Variation Filter (RBF-TVF) and Hybrid Total Variation Filter-Weighted Bilateral Filter (TVF-WBF) methods. The comparison revealed that the outcomes of the given approach are much sharper, clearer, and having the highest quality in comparison with other patch-based methods.

INDEX TERMS Image denoising, Bayesian patch-based method, PSNR, quaternion wavelet transform (QWT).

I. INTRODUCTION

Digital images are always susceptible to noise. The noise can be induced in the image during the image capture process due to the imaging sensor, transmission, or compression. Image denoising methods are used to produce a noise-free image similar to the original image. Image denoising has prime importance because further image processing methods immensely rely on the quality of the image. Image denoising methods are generally of the following two types: (i) Pixels-based denoising methods and (ii) Patch-based denoising methods. The pixel-based image denoising method works on a pixel-by-pixel approach i.e. one pixel at a time and then the process is further extended to the neighborhood defined in a specific kernel. On the contrary, the patch-based denoising method deals with the noisy image by dividing it into various patches or blocks. These patches are then treated independently, where the noise level in each patch is approximated and then removed to obtain a noise-free patch. This method is more effective than the former method because it performs a similar operation for the similar patches available in the image.

Wavelet transform (WT) is a noteworthy leap forward of the Fourier transform as it has extraordinary time-frequency restriction and numerous goal analysis highlights. Wavelet analysis has turned out to be a standout amongst the most valuable tools in pattern recognition, image processing, signal analysis, and numerous different fields. The key principle of the WT in image processing is to separate an image into different objectives. In particular, the principal image is separated into various spaces. Quaternion wavelet transform (QWT) is an extension of WT that is a combination of Quaternion Fourier Transform (QFT) and Discrete Wavelet Transform (DWT) [1]. Some of the applications of QWT has been found in numerous image denoising methods described in [2]–[4]. However, it is interesting to mention that all methods employing QWT are pixel-based methods and QWT with the patch-based method are yet to be explored.

The Bayesian Patch-based denoising methods are useful in many ways. Firstly, the result with the denoised image having smooth flat regions. In addition, the denoised image doesn't lose sharp edges and fine details. However, the method has

The associate editor coordinating the review of this manuscript and approving it for publication was Haiyong Zheng.

a shortcoming i.e. grouping and comparing of patches is not cost-effective in terms of computation time. However, this limitation is avoided if an image is transformed using QWT. Additionally, the QWT offers plentiful information about magnitude and phase. That motivates us to propose a novel method for image denoising in the Quaternion Wavelet domain using the Bayesian patch-based method. The proposed method combines the merit of the QWT and Bayesian patch-based method and provides an improved denoised image having better visual quality with less noise as compared to individual methods. The proposed algorithm is also compared with other traditional and patch-based denoising methods and the results are satisfactory. In addition, it is also found that the proposed method is computationally more cost-effective than other denoising methods, which is also a desirable feature for real-time image denoising.

The remaining work is organized in the following order: Section II outlines the literature review for QWT and patch-based denoising methods. A new state of the art algorithm has been proposed in Section III. Section IV is about the comparison between our proposed method and other denoising methods. section V will present the conclusion. Lastly, section VI will present the future work.

II. LITERATURE SURVEY

Marius [5] proposed the quaternion wavelet shape idea by using a real filter and the doubletree structure, using Bulow's quaternion analytic signal. Thomas [6] gives a clear depiction of nearby structures through shift-invariant greatness especially for 2D signals, for all intents and purposes identical to a standard DWT examination, and a three-point2-dimensional stage, passing on geometric data. Traversoni [7] used CWT and real wavelet transformation by quaternion Haar kernel and created discrete QWT and demonstrates a few usages in the image processing field. He and Bo [8] utilized matrix value work multi-resolution examination structure for back-to-back QWT and the work resulted in few properties. Eduardo [9] aggregates the perplexing and real wavelet transform and proposed a quaternion stage idea-based wavelet pyramid for a multi-resolution examination. Also, the optical stream estimation use of discrete QWT was suggested. Lam *et al.* [10] inspired by Quaternion Fourier Transform (QFT) and Bulow's quaternion information [6], developed double tree QWT in context of (*CWT*) determines the significance of three phases. Out of these three phases, one addresses the image texture feature while the other two address images of local displacement data. Geometric features of the image were checked using the image texture feature. For evaluating the confined geometrical structure of an image they established an effective and precise approach.

Mawardi [11] introduced quaternion-valued wavelets with respect to the duplex matrix-valued size and then employed quaternion scaling and wavelet capacities to get coefficients of high pass and low pass filters utilizing quaternion multi-resolution analysis (QMRA). Mawardi *et al.* [12] presented the continuous quaternion wavelet transform (CQWT). CQWT provided a suitability condition as well as the (right-sided) quaternion QFT. They also derived some fundamental characteristics, such as norm relation, inversion formula, and the inner product. Soulard and Philippe [13] proposed an improved version of QWT. The authors employed quaternion algebra and used actual 2D analytic wavelets to obtain sub-bands having a shift-invariant magnitude and a 3-angle phase. Min *et al.* [2], phenomenally examined the contemplation and traits of QWT in image denoising. It was found that under the Bayesian theory structure, Gauss distribution is utilized to exhibit QWT coefficients degree assignment to separate the important coefficients from the noisy ones. His preliminary outcomes exhibited that the proposed technique proved superior to various contemporary denoising methodologies. Haochen *et al.* [14] proposed a multi-focus color image fusion calculation with respect to QWT. His main objective was to deal with the issue of obscured images. A multi goals examination system was utilized using the quaternion wavelet transform. The predicted technique was differentiated and SWT and IHS strategies were used for target exercises i.e. image sharpness metric (ISM) and image differentiate metric (ICM). The multipart shading image gained from the converse quaternion wavelet transform resulted in outstanding outputs. Han [15] introduced an assessment standard for denoising implementation and a denoising system using an image wavelet threshold. The work explained quaternion with respect to wavelet transform area, hidden Markov tree was demonstrated for image denoising (Q-HMT), image denoising calculation for a non-Gaussian distribution model and a mixture statistical model. Results showed that the proposed study yielded improved performance. Fang-Fei *et al.* [16] a method by combining the QWT with the standard HMT display, according to new scheming without reshaping it, and had improved comprehension and an added advantage of the richer stage. The primary results demonstrated that the proposed scheme was better than other denoising estimations in terms of PSNR and image. Mohammed *et al.* [17] discussed the composition of multispectral images with strong auxiliary data and QWT capacity. The new representation of coefficients with respect to magnitude and three-stage points was an improvement. It also resulted in a better possibility of the logical signal to the image. Directivity and shift-invariant properties were also preserved. The method was tested in satellite image denoising. A multi-modal medical image fusion technique was proposed by Peng *et al.* [18] using a quaternion wavelet transform and efficient pulse coupled neural network. This method does not just apply on computed magnetic resonance (MR) and tomography (CT) images, but it can also be applied on multi-spectral MR images, proton density-weighted MR and CT images.

The two major image denoising methods based on patches are the Non-Local Means (NLM) and the Probabilistic Patch-Based (PPB) methods. Antoni *et al.* [19] the NLM

method as an enhancement to bilateral filter based on pixels. Rachid *et al.* [20] employed Markovian clustering as a better weight adjusting mechanism in the NLM method. Yue *et al.* [21] proposed an improved approach by adopting the [22] shrinkage estimator to adjust the weight in the NLM method. Rui and Xuan-Xuan [23] proposed an upgraded neighborhood method for the optimized weights of the NLM method. Asif and Mahmoud [24] presented a modified method of the NLM using a threshold step to decrease the similar patches before averaging the weight of the pixels. The PPB method was suggested as an advancement of the NLM method by Charles-Alban *et al.* [25]. Jorg and Vladimir [26] and Jorg and Tabelow [27] employed PPB for image denoising by using a weighted maximum probability estimation. Jun *et al.* [28] proposed a patch group-based learning method in which a Nonlocal Self-Similarity (NSS) model was learned from images that were later applied to noisy images for improved denoised images. Shuhang *et al.* [29] examined the Weighted Nuclear Norm Minimization (WNNM) method in which singular values were assigned to different weights. The resulting WNNM algorithm was applied to noisy images by manipulating non-local self-similarity. The proposed method provides more effective results as compared to other algorithms.

III. BAYESIAN PATCH-BASED IMAGE DENOISING USING QWT

In this work, a novel method is proposed for image denoising in the Quaternion Wavelet domain using the Bayesian patch-based method. Let I(i,i) represent noiseless image QWT coefficients and N(i,i) represents the noise QWT coefficients affected by Gaussian noise. Now the noisy image QWT coefficients can be written as

$$X(i,i) = I(i,i) + N(i,i) \tag{1}$$

The conditional distribution P(X| I) is given as

$$P(X|I) = \frac{1}{(2\pi\sigma^2)^{i^2/2}} e^{-\frac{\|I-X\|^2}{2\sigma^2}} \tag{2}$$

where I shows the noiseless image vector and σ is distribution variance.

The Bayesian expression for maximization of the posteriori distribution is given as

$$\hat{I}(X) = \mathrm{Arg}_I \max P(I|\, X) = \mathrm{Arg}_I \max P(X|I)P(I) \tag{3}$$

The expression can also be written as

$$I(X) = \mathrm{Arg}_I \max P(X|I)P(I) = \mathrm{Arg}_I \min \|I|X\|^2 + \frac{2\sigma^2}{T}E(I) \tag{4}$$

Here E(I) is the energy function and T is constant of Gibbs distribution.

In the proposed work, for image denoising, a patch model has been used instead of the Gibbs distribution based energy model. In this method, the patch is taken from the image. Let us take an example for more clarification, there is a noiseless patch A of dimension a × a in the image I and $\tilde{A}$ is the noise corrupted A, and the conditional distribution is given as;

$$P(\tilde{A}|\, A) = c.e^{-\frac{\|\tilde{A}|\, A\|^2}{2\sigma^2}} \tag{5}$$

Here A and $\tilde{A}$ represents a vector (patch) with a × a components and c represents cliques within the dimension of A.

The objective is to estimate A with the help of $\tilde{A}$ and maximization of P($\tilde{A}$| A). The target is achieved by using the Bayesian rule given as

$$P(\tilde{A}|A) = \frac{P(\tilde{A}|A)P(A)}{P(\tilde{A})} \tag{6}$$

TABLE 1. QWT based Bayesian Patch-based image denoising

Algorithm 1: QWT based Bayesian Patch-based Image Denoising

1. Transform the noisy image in QWT.
2. For all vectors $\tilde{A}$ of the noisy image X, determine the set $S(\tilde{A})$ of vectors $\tilde{\Lambda}$ similar to $\tilde{A}$.
3. Calculate the expectation $\bar{\tilde{A}} = \frac{1}{\#S(\tilde{A})} \sum_{\tilde{\Lambda}\in S(\tilde{A})} \tilde{\Lambda}$ and covariance matrix $C_{\tilde{A}} = \frac{1}{\#S(\tilde{A})-1} \sum_{\tilde{\Lambda}\in S(\tilde{A})} \left(\tilde{\Lambda}-\bar{\tilde{A}}\right)\left(\tilde{\Lambda}-\bar{\tilde{A}}\right)^t$.
4. Find the estimated denoised patches using Equation (19).
5. Determine the pixel value of the denoised image in QWT $\hat{I}(i,i)$ as an average of all values of denoised patches of the set $S(\tilde{A})$.
6. Apply the inverse QWT to the denoised estimated wavelet patches and achieve the denoised image.

FIGURE 1. Grayscale testing images.

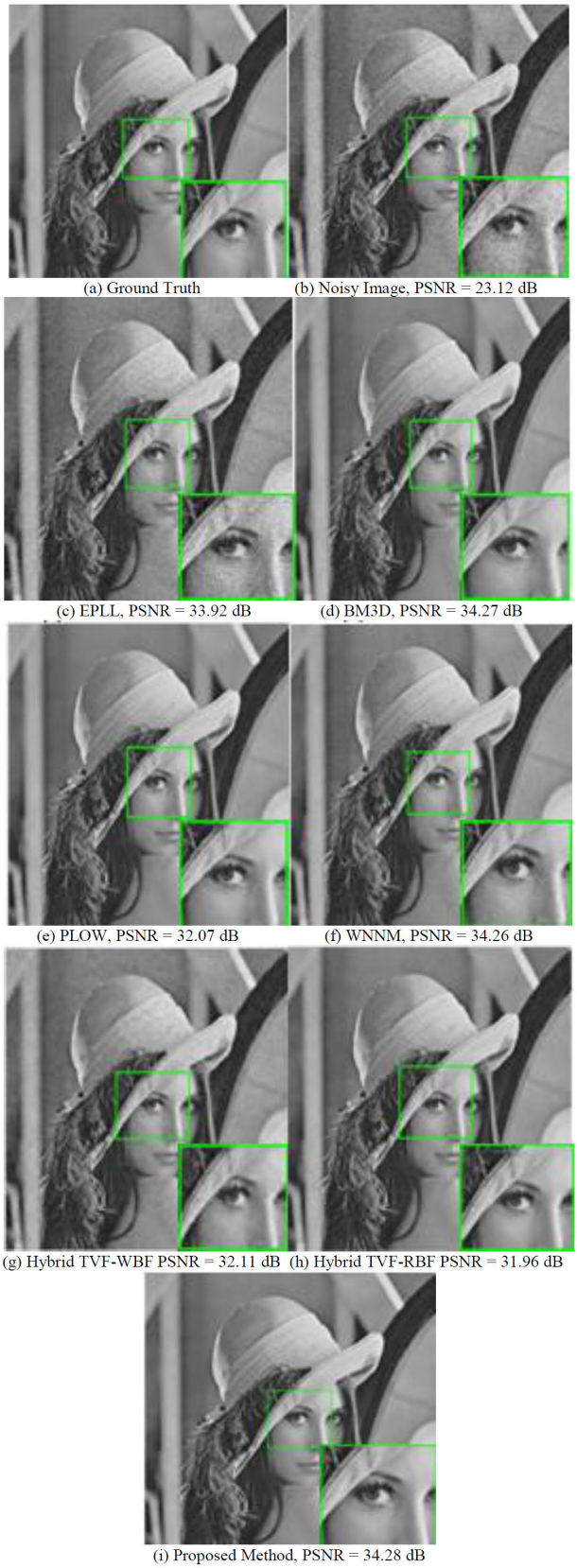

FIGURE 2. Subjective quality comparison of denoised images using different denoising methods on image Lena.

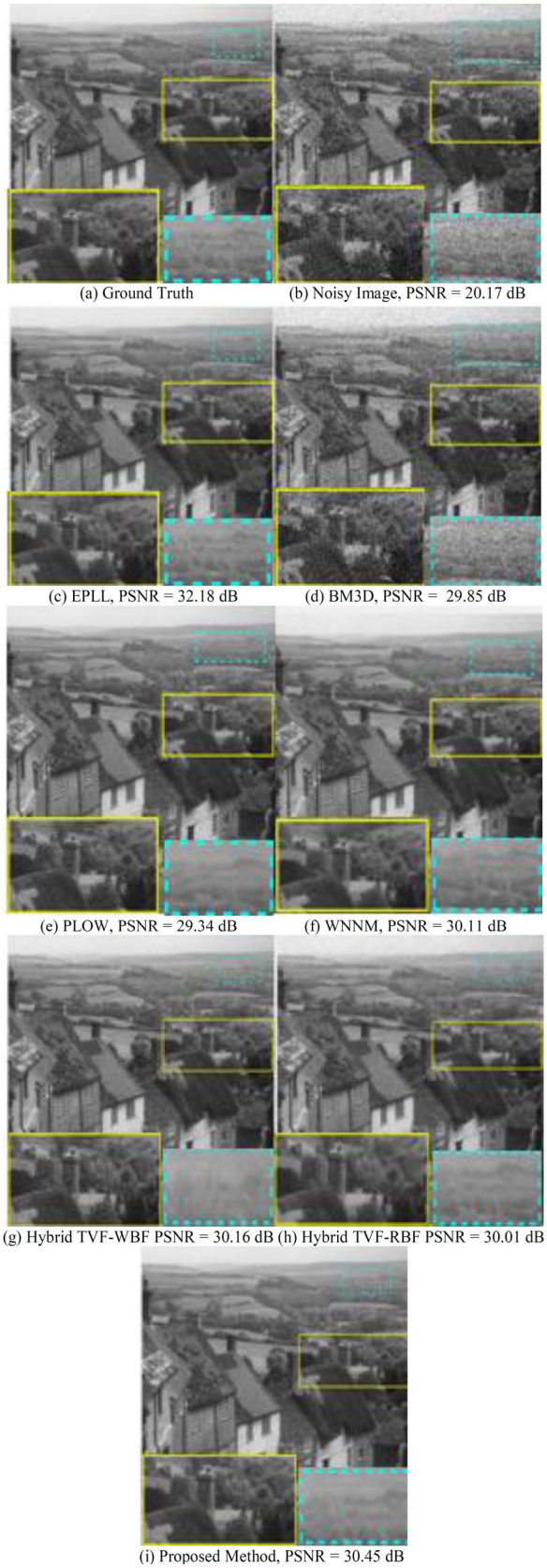

FIGURE 3. Subjective quality comparison of denoised images using different denoising methods on image Hill.

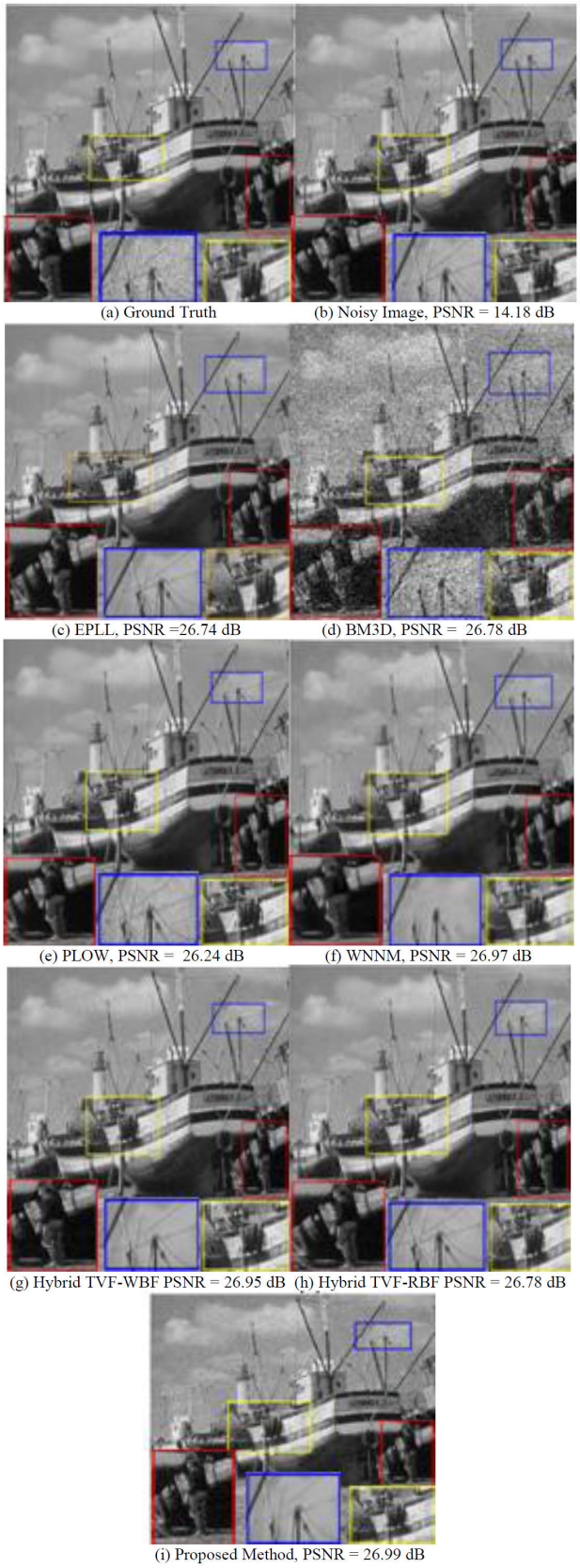

FIGURE 4. Subjective quality comparison of denoised images using different denoising methods on image Boat.

FIGURE 5. Subjective quality comparison of denoised images using different denoising methods on image Couple.

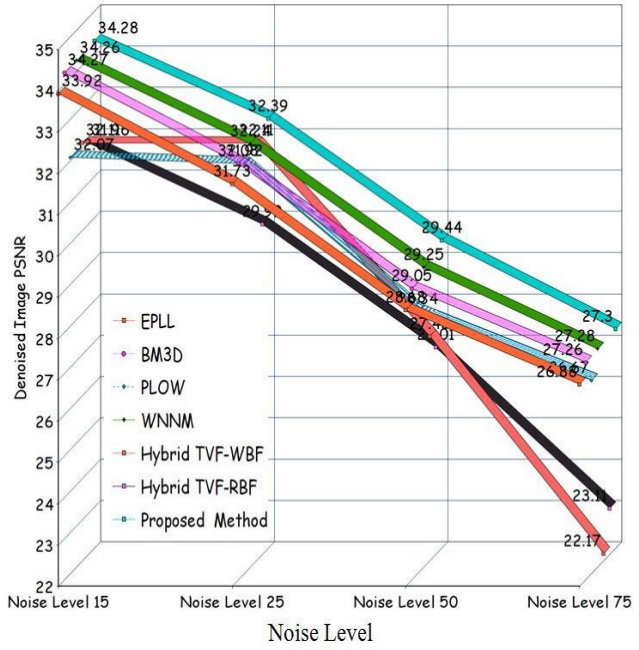

FIGURE 6. Graphical comparison of different denoising algorithms on image Lena.

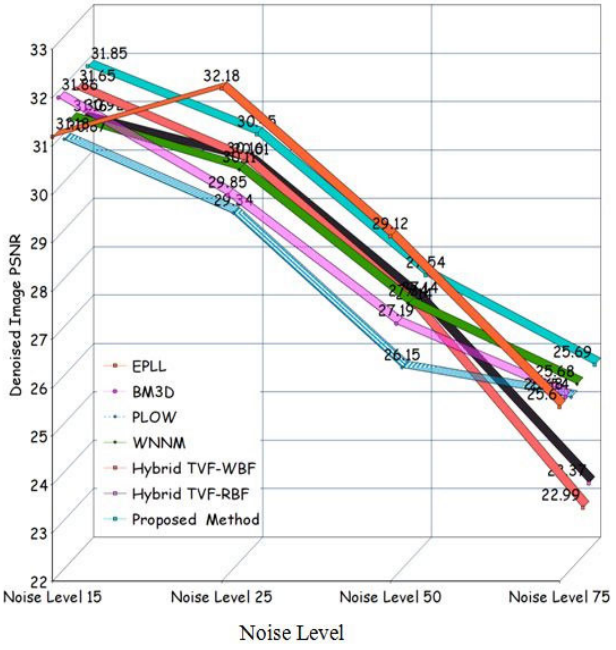

FIGURE 7. Graphical comparison of different denoising algorithms on image Hill.

The estimation is performed after the development of a probability model for A from image. In addition, the model for vector $\tilde{A}$ is developed by grouping all vectors in an image similar to $\tilde{A}$. It is also assumed that there are Λ vectors similar to A are also Gaussian in nature with covariance matrix C_A and mean $\overline{A}$. This implies

$$P(\Lambda) = c.e^{-\frac{(\Lambda-\bar{A})^t C_A^{-1}(\Lambda-\bar{A})}{2}} \tag{7}$$

For each observed value of $\tilde{A}$, we can derive the following using Equations (2) and (6):

$$\max_A P(A|\tilde{A}) \Leftrightarrow \max_A P(\tilde{A}|A)P(A) \tag{8}$$

$$\Leftrightarrow \max_A e^{-\frac{\|A-\tilde{A}\|^2}{2\sigma^2}} e^{-\frac{(A-\bar{A})^t C_A^{-1}(A-\bar{A})}{2}} \tag{9}$$

$$\Leftrightarrow \min_A \frac{\|A-\tilde{A}\|^2}{\sigma^2} + (A-\bar{A})^t C_A^{-1}(A-\bar{A}) \tag{10}$$

Therefore, we can estimate $\bar{A}$ and can determine the vectors $\tilde{\Lambda}$ similar to $\tilde{A}$. The covariance matrix $C_{\tilde{A}}$ can be determined in this regard which is given as

$$\begin{aligned} C_{\tilde{A}} &= C_A + \sigma^2 I \\ E\tilde{\Lambda} &= \bar{A} \end{aligned} \tag{11}$$

It is worth mentioning here that all vectors are searched to find vectors similar to $\tilde{A}$ keeping in view with an assumption that the search is performed in a distance slightly larger than the expected distance caused by noise. Based on the above calculation and assumption, Maximum A Posteriori (MAP) estimation is used with Equation (11) to find the following minimization expression:

$$\max_A P(A|\tilde{A}) \Leftrightarrow \min_A \frac{\|A-\tilde{A}\|^2}{\sigma^2} + (A-\bar{\tilde{A}})^t \left(C_{\tilde{A}} - \sigma^2 I\right)^{-1} (A-\bar{\tilde{A}}) \tag{12}$$

The differentiation of Equation (12) w.r.t A with equal to zero results in

$$A - \tilde{A} + \sigma^2 (C_{\tilde{A}} - \sigma^2 I)^{-1}(A - \bar{\tilde{A}}) = 0 \tag{13}$$

It is clear that $I + \sigma^2 \left(C_{\tilde{A}} - \sigma^2 I\right)^{-1} = \left(C_{\tilde{A}} - \sigma^2 I\right)^{-1} C_{\tilde{A}}$, therefore,

Equation (13) results in

$$\left(C_{\tilde{A}} - \sigma^2 I\right)^{-1} C_{\tilde{A}} A = \tilde{A} + \sigma^2 \left(C_{\tilde{A}} - \sigma^2 I\right)^{-1} \bar{\tilde{A}} \tag{14}$$

Thus, we can get A as

$$A = C_{\tilde{A}}^{-1}(C_{\tilde{A}} - \sigma^2 I)\tilde{A} + \sigma^2 C_{\tilde{A}}^{-1} \bar{\tilde{A}} \tag{15}$$

$$= \tilde{A} + \sigma^2 C_{\tilde{A}}^{-1}(\bar{\tilde{A}} - \tilde{A}) \tag{16}$$

$$= \bar{\tilde{A}} + \left[I - \sigma^2 C_{\tilde{A}}^{-1}\right](\tilde{A} - \bar{\tilde{A}}) \tag{17}$$

$$= \bar{\tilde{A}} + \left[C_{\tilde{A}} - \sigma^2 I\right] C_{\tilde{A}}^{-1}(\tilde{A} - \bar{\tilde{A}}) \tag{18}$$

Therefore, it is derived that a denoised vector or patch $\hat{A}$ in the QWT domain can be obtained using an estimated vector $\tilde{A}$ using the following expression

$$\hat{A} = \bar{\tilde{A}} + \left[C_{\tilde{A}} - \sigma^2 I\right] C_{\tilde{A}}^{-1}(\tilde{A} - \bar{\tilde{A}}) \tag{19}$$

TABLE 2. PSNR comparison of different denoising algorithms on image Lena.

Standard Images	Lena	Hill	Boat	Camera Man	House	Peppers	Monarch	Airplane	Parrot	Barbara	Man	Couple
Noise Level	Noise Standard Deviation σ 15											
EPLL [30]	33.92	31.18	31.93	31.85	34.17	32.64	32.10	31.19	31.42	31.38	32.00	31.93
BM3D [31]	34.27	31.86	32.14	31.91	34.94	32.70	35.85	31.07	31.37	33.10	31.93	32.11
PLOW [32]	32.07	30.87	32.00	30.97	33.99	31.67	31.84	31.01	30.98	32.02	30.37	31.57
WNNM [29]	34.26	31.16	32.27	32.17	35.13	32.99	32.71	31.39	31.62	33.60	32.11	32.17
Hybrid TVF-WBF [33]	32.11	31.65	31.99	32.15	33.03	31.04	32.02	31.30	30.99	32.16	31.44	31.99
Hybrid TVF-RBF [34]	31.96	30.92	30.67	31.00	30.17	30.16	30.01	30.05	30.06	30.16	31.22	31.09
Proposed Method	**34.28**	**31.85**	**32.57**	**33.90**	**35.95**	**33.14**	**35.88**	**31.67**	**31.94**	**33.91**	**32.54**	**32.19**

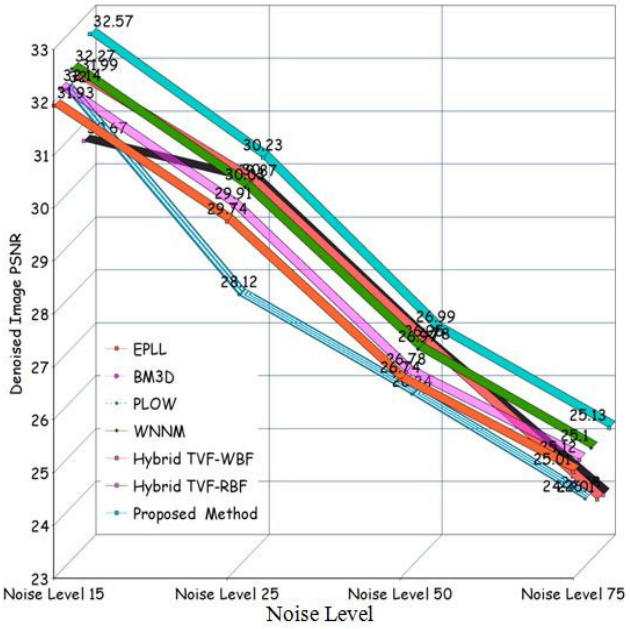

FIGURE 8. Graphical comparison of different denoising algorithms on image Boat.

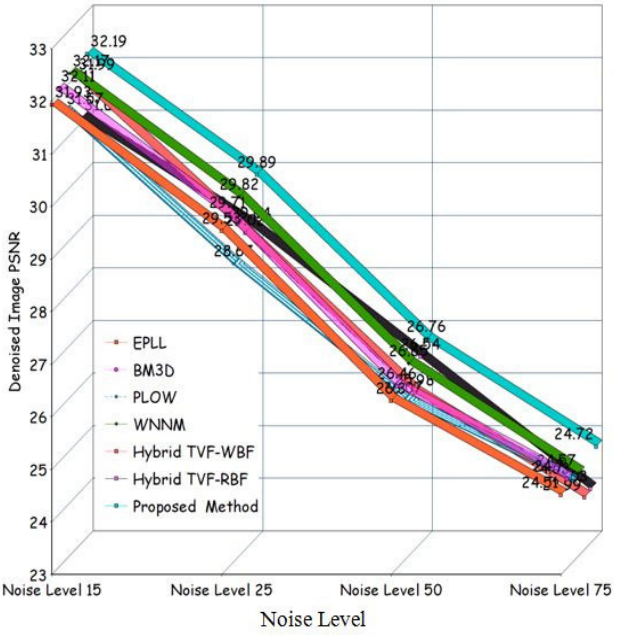

FIGURE 9. Graphical comparison of different denoising algorithms on image Couple.

And a set of all such patches can be denoised to get the denoised image in the QWT domain. The algorithm for the proposed QWT based Bayesian patch-based image denoising is given in Table 1.

IV. RESULTS

We tested the adequacy of our proposed algorithm with six benchmark denoising algorithms, i.e. the EPLL [30], BM3D [31], PLOW [32] and WNNM [29], Hybrid TVF-WBF [33], and Hybrid TVF-RBF [34] methods.

For our experiments, we used 12 different grayscale images from two different datasets [35], [36] that are shown in Figure 1. Original image "Lena", "Hill" "Boat" and "Couple" can be found in Figure 2(a), 3(a) 4(a) and 5(a).

Test images have size 256 × 256, 512 × 512 and 1024 × 1024 pixels having low, medium, and high complexity respectively. For our experiments, we utilized white gaussian noise (WGN) with zero mean and variances σ. Noisy images using noise level 15, 25, 50, and 75 can be found in Figure 2(b), 3(b), 4(b) and 5(b). Denoised outputs images of the different state of the art can be found in Figure 2(c) to 2(h), 3(c) to 3(h), 4(c) to 4(h) and 5(c) to 5(h). Improved denoised images, the patch-based method using QWT can be found in Figure 2(i), 3(i), 4(i) and 5(i). From experimental results, it can be seen that the reconstructed images have better visual quality. It is quite evident that pixel-wise processing mechanisms BM3D bring smearing-mud like objects.

TABLE 3. PSNR comparison of different denoising algorithms on image Hill.

Standard Images	Lena	Hill	Boat	Camera Man	House	Peppers	Monarch	Airplane	Parrot	Barbara	Man	Couple
Noise Level	Noise Standard Deviation σ 25											
EPLL [30]	31.73	32.18	29.74	29.26	32.17	30.17	29.39	28.61	28,95	28.61	29.66	29.53
BM3D [31]	32.08	29.85	29.91	29.45	32.86	30.16	29.25	28.42	28.93	30.71	29.62	29.71
PLOW [32]	31.92	29.34	28.12	27.93	32.70	26.56	27.06	27.44	26.67	28.45	28.08	28.67
WNNM [29]	32.24	30.11	30.03	29.64	33.22	30.42	29.84	28.69	29.15	31.24	29.76	29.82
Hybrid TVF-WBF [33]	32.11	30.16	30.00	29.13	32.18	30.11	29.02	28.67	28.99	29.92	29.25	29.02
Hybrid TVF-RBF [34]	29.99	30.01	29.87	29.77	29.98	29.92	29.93	28.99	29.15	29.24	29.37	29.04
Proposed Method	**32.39**	**30.45**	**30.23**	**29.74**	**33.38**	**30.71**	**29.97**	**28.83**	**29.98**	**31.73**	**29.81**	**29.89**

TABLE 4. PSNR comparison of different denoising algorithms on image Boat.

Standard Images	Lena	Hill	Boat	Camera Man	House	Peppers	Monarch	Airplane	Parrot	Barbara	Man	Couple
Noise Level	Noise Standard Deviation σ 50											
EPLL [30]	28.68	29.12	26.74	26.10	29.12	26.80	25.94	25.31	25.95	24.83	26.79	26.30
BM3D [31]	29.05	27.19	26.78	26.12	29.69	26.68	25.82	25.10	25.90	27.23	26.81	26.46
PLOW [32]	28.34	26.15	26.24	25.06	28.34	26.15	25.00	25.09	25.18	25.39	26.13	26.07
WNNM [29]	29.25	27.34	26.97	26.45	30.33	26.95	26.32	25.42	26.14	27.79	26.94	26.65
Hybrid TVF-WBF [33]	27.43	27.14	26.95	26.11	29.01	25.99	25.99	25.12	26.03	26.99	26.01	25.98
Hybrid TVF-RBF [34]	27.01	27.14	26.78	26.02	28.45	26.11	26.93	25.01	25.76	26.18	26.94	26.54
Proposed Method	**29.44**	**27.54**	**26.99**	**26.78**	**29.34**	**26.98**	**26.93**	**25.53**	**26.15**	**27.92**	**26.97**	**26.76**

TABLE 5. PSNR comparison of different denoising algorithms on image Couple.

Standard Images	Lena	Hill	Boat	Camera Man	House	Peppers	Monarch	Airplane	Parrot	Barbara	Man	Couple
Noise Level	Noise Standard Deviation σ 75											
EPLL [30]	26.88	25.60	25.01	24.29	27.09	27.15	23.88	26.14	23.17	22.94	25.26	24.51
BM3D [31]	27.26	25.68	25.12	24.33	27.51	24.73	24.95	25.12	25.18	25.12	25.32	24.70
PLOW [32]	26.67	25.54	24.26	23.87	26.34	24.17	23.03	26.04	23.23	22.12	24.99	24.53
WNNM [29]	27.28	25.68	25.10	24.30	27.39	24.56	24.45	25.01	25.03	25.00	25.14	24.57
Hybrid TVF-WBF [33]	22.17	22.99	24.01	23.55	23.99	24.00	23.98	24.06	25.17	23.93	24.15	23.99
Hybrid TVF-RBF [34]	23.11	23.37	23.98	24.01	23.68	23.99	24.14	25.02	24.44	24.11	24.97	24.03
Proposed Method	**27.30**	**25.69**	**25.13**	**24.43**	**27.60**	**24.78**	**24.97**	**25.14**	**25.19**	**25.16**	**25.36**	**24.72**

The results clearly show that our proposed technique produces a sharper denoising output that has the best visual quality. BM3D aims at the pointwise optimal reconstruction of the noise-corrupted signal that favors the point-wise PSNR calculation. Our Proposed algorithm aims at better image quality both numerically and visually. Furthermore, it also offers reduced computational cost.

Table 2 to 5 illustrates the comparative results in PSNR for standard images shown in Figure 1 at different noise levels. Through observing these results, it is quite noticeable that

TABLE 6. Run time (in seconds) of different methods on images of size 256 × 256 (Lena), 512 × 512 (Boat) and 1024 × 1024 (Camera Man) with noise level 25 and 50.

Image Size	Noise Level	EPLL [30]	BM3D [31]	PLOW [32]	WNNM [29]	Hybrid TVF-WBF [33]	Hybrid TVF-RBF [34]	Proposed Method
256x256	25	25.51	1.47	4.01	203.4	1.45	1.39	**0.98**
512x512	50	45.59	5.42	19.03	773.9	5.48	5.33	**4.02**
1024x1024	50	422.11	23.53	66.20	2537.2	16.90	15.78	**16.32**

our proposed algorithm has excellent PSNR results when compared to other image denoising methods. It can be also observed that the PSNR value of the proposed method is better at different noise levels whereas other methods perform well at low to medium noise level.

Figures 6 to 9 present the graphical comparisons of different image denoising techniques. The X-axis shows noise levels from 10 to 75, while Y-axis shows denoised image PSNR.

A. RUN TIME

These experiments were conducted on an Intel Core i7-3610QM 3rd Generation PC, CPU 2.3 GHz, with window 7, 64-bit operating system. It is undoubtedly visible that the proposed algorithm has up to par performance with less complexity and improved implementation time. The comparison of the average run time of all algorithms on the given data set is presented in Table 6 for image size 256 × 256, 512 × 512 and 1024 × 1024 with noise level 25 and 50.Tabular data also shows that our proposed algorithm run time is fast as compared to other methods. Finally, experimental results, tables, and graphical comparison demonstrate that our proposed algorithm has high-quality PSNR and fast implementation time results as compared to other image denoising methods.

V. CONCLUSION

The article proposed a Bayesian patch-based image denoising method using QWT. The article provided a detailed literature review of image denoising using quaternion and QWT. Afterward detail about the proposed algorithm is also provided. Experimental outcomes demonstrate that the denoised images have the finest visual quality with comparison to other state-of-the-art denoising algorithms. Trial results likewise demonstrate that the proposed strategy exhibits great execution as far as both subjective measures and objective measures of PSNR. In addition, PSNR results are additionally attained at low computations. The proposed algorithm run time is also fast as compared to other methods.

VI. FUTURE WORK

This article is proposing the new Bayesian Patch-based image denoising algorithm using Quaternion Wavelet Transform (QWT). As for our future work, we will highly recommend to use this technique with different types of filter and mixed noises and examine performance.

REFERENCES

[1] A. Vyas and J. Paik, "Applications of multiscale transforms to image denoising: Survey," in *Proc. Int. Conf. Electron., Inf., Commun. (ICEIC)*, Jan. 2018, pp. 1–3.
[2] M. Yin, W. Liu, J. Shui, and J. Wu, "Quaternion wavelet analysis and application in image denoising," *Math. Problems Eng.*, vol. 2012, Oct. 2012, Art. no. 493976.
[3] Y. Liu, J. Jin, Q. Wang, and Y. Shen, "Phase-preserving speckle reduction based on soft thresholding in quaternion wavelet domain," *J. Electron. Imag.*, vol. 21, no. 4, Oct. 2012, Art. no. 043009.
[4] P. Chai, X. Luo, and Z. Zhang, "Image fusion using quaternion wavelet transform and multiple features," *IEEE Access*, vol. 5, pp. 6724–6734, 2017.
[5] M. Mitrea, *Clifford Wavelets, Singular Integrals, and Hardy Spaces* (Lecture Notes in Mathematics). Berlin, Germany: Springer-Verlag, 1994.
[6] T. B. Ulow, "Hypercomplex spectral signal representations for the processing and analysis of images," Inst. Inform. Practical Math., Christian Albrechts Universitat Kiel, Kiel, Germany, Tech. Rep. TR_9903, Aug. 1999. [Online]. Available: https://www.uni-kiel.de/journals/receive/jportal_jparticle_00000190
[7] L. Traverson, "Image analysis using quaternion wavelets," in *Geometric Algebra With Applications in Science and Engineering*. Boston, MA, USA: Springer, 2001, pp. 326–345.
[8] H. Jianxun and Y. Bo, "Continuous wavelet transforms on the space L^2 (R, H; dx)," *Appl. Math. Lett.*, vol. 17, no. 1, pp. 111–121, 2004.
[9] E. Bayro-Corrochano, "The theory and use of the quaternion wavelet transform," *J. Math. Imag. Vis.*, vol. 24, no. 1, pp. 19–35, Dec. 2005.
[10] W. Lam Chan, H. Choi, and R. G. Baraniuk, "Coherent multiscale image processing using dual-tree quaternion wavelets," *IEEE Trans. Image Process.*, vol. 17, no. 7, pp. 1069–1082, Jul. 2008.
[11] B. Mawardi, "Construction of quaternion valued wavelets," *Matematika*, vol. 26, no. 1, pp. 107–114, 2010.
[12] M. Bahri, R. Ashino, and R. Vaillancourt, "Two-dimensional quaternion Fourier transform of type II and quaternion wavelet transform," in *Proc. Int. Conf. Wavelet Anal. Pattern Recognit.*, Jul. 2012, pp. 359–364.
[13] R. Soulard and P. Carré, "Quaternionic wavelets for texture classification," *Pattern Recognit. Lett.*, vol. 32, no. 13, pp. 1669–1678, Oct. 2011.
[14] H. Pang, M. Zhu, and L. Guo, "Multifocus color image fusion using quaternion wavelet transform," in *Proc. 5th Int. Congr. Image Signal Process. (CISP)*, Oct. 2012, pp. 543–546.
[15] H. Tianfeng, "The method of quaternions wavelet image denoising," *Int. J. Signal Process., Image Process. Pattern Recognit.*, vol. 7, no. 4, pp. 325–334, Aug. 2014.
[16] F.-F. Yu, X. Liu, and L.-G. Sun, "Image denoising based on quaternion wavelet Q-HMT model," in *Proc. 33rd Chin. Control Conf.*, Jul. 2014, pp. 6279–6282.
[17] M. Kadiri, M. Djebbouri, and P. Carré, "Magnitude-phase of the dual-tree quaternionic wavelet transform for multispectral satellite image denoising," *EURASIP J. Image Video Process.*, vol. 2014, no. 1, pp. 1–16, Aug. 2014.
[18] P. Geng, X. Sun, and J. Liu, "Adopting quaternion wavelet transform to fuse multi-modal medical images," *J. Med. Biol. Eng.*, vol. 37, no. 2, pp. 230–239, Mar. 2017.
[19] B. Antoni, C. Bartomeu, and M. J. Michel, "A non-local algorithm for image denoising," in *Proc. IEEE Comput. Soc. Conf. Comput. Vis. Pattern Recognit. (CVPR)*, vol. 2, Jun. 2005, pp. 60–65.
[20] R. Hedjam, R. F. Moghaddam, and M. Cheriet, "Markovian clustering for the non-local means image denoising," in *Proc. 16th IEEE Int. Conf. Image Process. (ICIP)*, Nov. 2009, pp. 3877–3880.
[21] Y. Wu, B. Tracey, P. Natarajan, and J. P. Noonan, "James-stein type center pixel weights for non-local means image denoising," *IEEE Signal Process. Lett.*, vol. 20, no. 4, pp. 411–414, Apr. 2013.

[22] W. James and S. Charles, "Estimation with quadratic loss," in *Proc. Berkeley Symp. Math. Statist. Probab.*, vol. 1, 1961, pp. 3610–3379.
[23] R. Lai and X.-X. Dou, "Improved non-local means filtering algorithm for image denoising," in *Proc. 3rd Int. Congr. Image Signal Process. CISP*, Oct. 2010, pp. 720–722.
[24] K. Asif and M. R. El-Sakka, "Adaptive non-local means using weight thresholding," in *Proc. Int. Joint Conf. Comput. Vis., Imag. Comput. Graph.*, vol. 693, 2017, pp. 493–514.
[25] C.-A. Deledalle, L. Denis, and F. Tupin, "Iterative weighted maximum likelihood denoising with probabilistic patch-based weights," *IEEE Trans. Image Process.*, vol. 18, no. 12, pp. 2661–2672, Dec. 2009.
[26] P. Jorg and S. Vladimir, "Propagation-separation approach for local likelihood estimation," *Probab. Theory Related Fields*, vol. 135, no. 3, pp. 335–362, 2006.
[27] P. Jorg and K. Tabelow, "Adaptive smoothing of digital images: The R package adimpro," *J. Stat. Softw.*, vol. 19, no. 1, pp. 1–17, 2007.
[28] X. Jun, Z. Lei, Z. Wangmeng, Z. David, and F. Xiangchu, "Patch group based nonlocal self-similarity prior learning for image denoising," in *Proc. IEEE Int. Conf. Comput. Vis. (ICCV)*, Dec. 2015, pp. 7–13.
[29] S. Gu, L. Zhang, W. Zuo, and X. Feng, "Weighted nuclear norm minimization with application to image denoising," in *Proc. IEEE Conf. Comput. Vis. Pattern Recognit.*, Jun. 2014, pp. 2862–2869.
[30] D. Zoran and Y. Weiss, "From learning models of natural image patches to whole image restoration," in *Proc. Int. Conf. Comput. Vis.*, Nov. 2011, pp. 479–486.
[31] D. Kostadin, F. Alessandro, K. Vladimir, and K. O. Egiazarian, "Image denoising by sparse 3-D transform domain collaborative filtering," *IEEE Trans. Image Process.*, vol. 16, no. 8, pp. 2080–2095, 2007.
[32] P. Chatterjee and P. Milanfar, "Patch-based near-optimal image denoising," *IEEE Trans. Image Process.*, vol. 21, no. 4, pp. 1635–1649, Apr. 2012.
[33] R. Ali, P. Yunfeng, and S. K. Gupta, "Fusion of total variation filter and weighted bilateral filter in image denoising," *Int. J. u-e-Service, Sci. Technol.*, vol. 11, no. 1, pp. 17–32, Mar. 2018, doi: 10.14257/ijunesst.2018.11.1.02.
[34] A. Rashid, Y. Peng, T. I. Muhammad, and I. Muhammad, "Combination of total variation and robust bilateral filter in image denoising," in *Proc. Frontiers Artif. Intell. Appl., Inf. Technol. Intell. Transp. Syst.*, vol. 314, 2019, pp. 127–141.
[35] ImageProcessingPlace.com. *Image Database*. Accessed: Jul. 19, 2019. [Online]. Available: http://imageprocessingplace.com/root_files_V3/image_databases.htm
[36] CVG UGR Database. *Image Database*. Accessed: Jul. 18, 2019. [Online]. Available: http://decsai.ugr.es/cvg/dbimagenes/

RASHID ALI received the master's degree in signal and information processing from Northwestern Polytechnical University, Xi'an, China, in 2015. He is currently a Ph.D. Researcher with the School of Computer and Communication Engineering, University of Science and Technology Beijing (USTB), Beijing, China. He has published one book in Lambert Academic Publishing Germany. He has several publications in international journals and international conferences indexed by SCI and EI. His research interest broadly include the areas of image processing, image denoising, image enhancement, and image compression.

PENG YUNFENG (Member, IEEE) received the B.E. degree from the Nanjing University of Science and Technology, in 1996, and the M.S. degree from the Kunming University of Science and Technology, in 2003, and the Ph.D. degree from Shanghai Jiaotong University, in 2007. He is currently a full-time Professor with the Department of Communication and Information Engineering, University of Science and Technology Beijing, Beijing, China. His research interests include image processing and network communications.

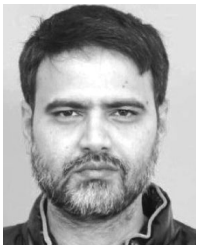

ROOH UL AMIN received the B.E. degree in industrial electronics from NED UET, in 2003, the M.S. degree in system engineering from PIEAS, in 2005, and the Ph.D. degree from Northwestern Polytechnical University, in 2017. He is currently working at the Faculty of Telecommunication & Information Engineering, University of Engineering and Technology, Taxila, Pakistan. His research interest broadly include the areas of control engineering, intelligent systems, stochastic processes, and image processing. He has several publications in international journals and conferences and ISI, and Scopus indexed journals. He is also a Reviewer of several international journals and international conferences.